Elementary Steps in Heterogeneous Catalysis**

By Gerhard Ertl*

Despite the great importance of heterogeneous catalysis, research in this field has long been characterized by its empiricism. Now, however, thanks to the rapid development of methods in surface physics, the elementary steps can be identified at the atomic level and the underlying principles understood. Defined single crystal surfaces are employed as models, based on the analysis of the surfaces of 'real' catalysts. Direct images, with atomic resolution, can be obtained using scanning tunneling microscopy, while electron spectroscopic methods yield detailed information on the bonding state of adsorbed species and the influence of catalyst additives (promotors) upon them. The successful application of this approach is illustrated with reference to the elucidation of the mechanism of ammonia synthesis. The catalyst surface is usually transformed under reaction conditions, and, as the processes involved are far-removed from equilibrium, such transformations can lead to intrinsic spatial and temporal self-organization phenomena. In this case, the reaction rate may not remain constant under otherwise invariant conditions but will change periodically or exhibit chaotic behavior, with the formation of spatial patterns on the catalyst surface.

1. Introduction

The term 'catalysis,' originally coined by *Berzelius* in 1835 was itself occasionally the subject of considerable controversy up to the end of the 19th century, until *W. Ostwald* was finally able to clarify its relationship to the rate of chemical reaction. How exactly a catalyst works remains, however, something of a mystery to this day. It is for this reason that the strategy of extensive catalyst screening for technical applications, introduced by *A. Mittasch* around 1909, still finds widespread use today. Between 1909 and 1912 *Mittasch* carried out about 6500 activity determinations on around 2500 different catalysts, as part of the development of the Haber-Bosch process.[1] His endeavors met with striking success—the catalyst composition he developed is still being used industrially today, in largely unaltered form. For *Fritz Haber* the catalyst question had been solved with the discovery of the catalytic activity of osmium and uranium. It soon became evident, however, that the large-scale application of such materials was hardly a realistic proposition.

Mittasch was inspired by the idea "in the catalytic production of ammonia some kind of intermediate nitrides are formed, even if of very labile nature."[2] Following the discovery of the increased activity of mixed catalysts (promotor effect), first described in a patent dated January 9, 1910,[3] he speculated, "that the nitrogen is taken up by one component and the hydrogen by another in a labile form and activated. As a result of the intimate association of both components, the strongly reactive nitrogen then unites with the similar form of the hydrogen, thus readily forming ammonia, which is then emitted". He admitted, somewhat meekly, however, "that this is just a rough model, which in theoretical terms leaves us somewhat out on a limb."[4]

Apart from the intellectual curiosity expressed in this statement, *Mittasch* had recognized that, despite the success achieved, the situation would remain unsatisfactory in practical terms as long as a better comprehension of the fundamental atomic processes was lacking. Only such an approach would one day enable an optimal catalyst to be 'tailored' for a desired application.

Nevertheless, one should always bear in mind that, for practical purposes, not only the intrinsic chemical activity but also other properties, such as the diffusive behavior, the strength, mechanical stability etc., can be decisive factors. This further complicates the situation and ensures that for a given reaction *the* catalyst is usually a pipe dream.

Thanks to the development of powerful techniques in the area of surface physics and the accompanying theoretical advances, considerable progress has been made in the last few years towards answering the major questions concerning the characterization of the elementary processes underlying a catalytic reaction. This paper will report some aspects of the advances which have been achieved as examples.

Since industrial reactions proceed on complex catalysts and under conditions, e.g. high pressure, that rule out the direct in-situ application of most of the experimental methods mentioned, the following stepwise approach has proved both expedient and successful:

1. The surface properties, especially chemical composition and the distribution of various elements, may deviate considerably from those of the bulk. It is thus first necessary to characterize the surface, and in particular the 'active centers' of a catalyst, in as much detail as possible. The so-called 'pressure gap' mentioned before can present special difficulties, as an examination under actual reaction conditions is problematical. Simplified model systems for the structure and chemical composition are therefore enlisted, above all to permit the systematic variation of these parameters. The most convenient systems for this purpose are well-defined, single crystal surfaces. Their use naturally introduces a 'materials gap', meaning one subsequently has to check, in each case, the extent to which the properties of the 'real' catalyst agree with those of the model system.

2. The essence of the surface science approach is the study of the energetics and dynamics of the interactions between the molecules participating in the reaction and the model

[*] Prof. Dr. G. Ertl
Fritz-Haber-Institut der Max-Planck-Gesellschaft
Faradayweg 4-6, 1000 Berlin 33

[**] From a paper presented at the awarding of the A.-Mittasch Medal during a colloquium celebrating the 125th. anniversary of the founding of BASF on September 24, 1990 in Ludwigshafen (FRG).

surfaces mentioned and structures of the chemisorbed phases formed thereby. On this basis, one determines the microscopic reaction mechanism and the kinetics of the elementary steps.

3. Information on the reaction mechanism, which should be as complete as possible, enables one, in principle, to develop a kinetic scheme for calculating the steady state reaction rate as a function of external parameters, such as temperature, partial pressure, etc. When translating the results to industrial conditions, the agreement between the calculated (i.e. predicted) and experimental conversions is the yardstick for success.

Although the strategy outlined has up to now only been realized thoroughly and successfully in two instances (CO oxidation and ammonia synthesis), these have demonstrated its basic soundness. Quite apart from this, even clarification of individual aspects can provide a rich vein of important data relevant to practical applications.

2. From "Real" Catalysts to Single Crystal Surfaces

Industrial catalysts are, as a rule, very complex systems in terms of the structure and chemical composition of their surfaces. This is evident in Figure 1, which depicts a scanning

Fig. 1. Scanning electron microscope image of the surface topography of a commercial ammonia synthesis catalyst [5].

electron microscope image of the BASF ammonia synthesis catalyst S6-10.[5] The topography exhibits a labyrinth of catalyst material and pores with a diameter of typically several hundred angstroms, which is reflected in the relatively high specific area of around 15 $m^2 g^{-1}$. The source material, magnetite (Fe_3O_4), which is reduced to metallic iron during the activation process, contains low concentrations of Al_2O_3 (+ CaO) and K_2O as additives. As *Mittasch* discovered,[3] these 'promotors' make an important contribution toward raising the activity. During the course of complex solid-state chemical reactions associated with catalyst activation,[6] aluminum, in the form of its ternary oxides fabricates a kind of framework, which prevents the Fe particles from sintering together, and thus plays the role of a 'structural' promotor.

The rather inhomogeneous distribution of the various elements over the catalyst surface can be seen from Figure 2 in the series of Auger electron spectra taken at different locations. In the case of No. 1, a catalytically active site with

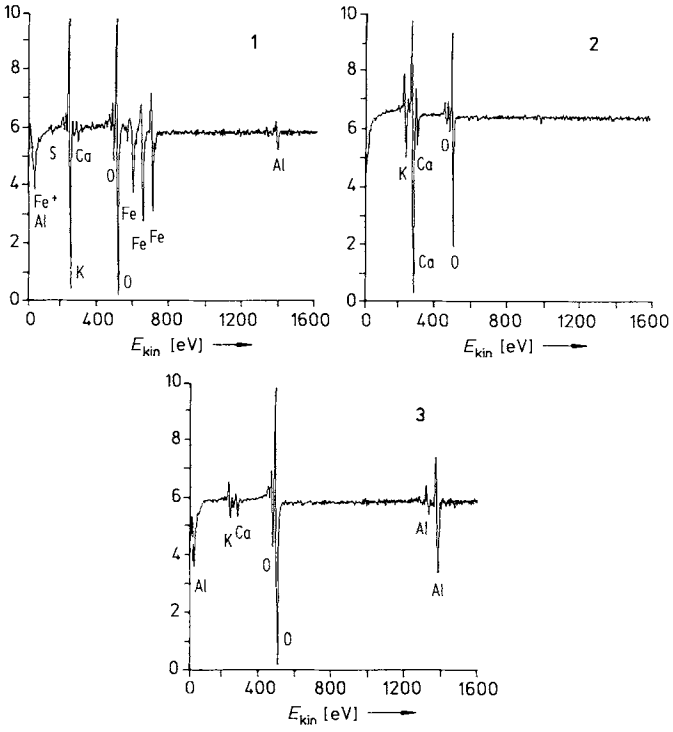

Fig. 2. Auger electron spectra from various locations on the surface of an ammonia synthesis catalyst [5]. E_{kin} = kinetic energy of the electrons.

considerable concentrations of Fe and K (+ O) is analyzed, while No. 2 largely consists of CaO, and No. 3 of Al_2O_3. The laterally resolved chemical composition of the surface is illustrated in 'Auger maps' in Figure 3. Remarkably, potassi-

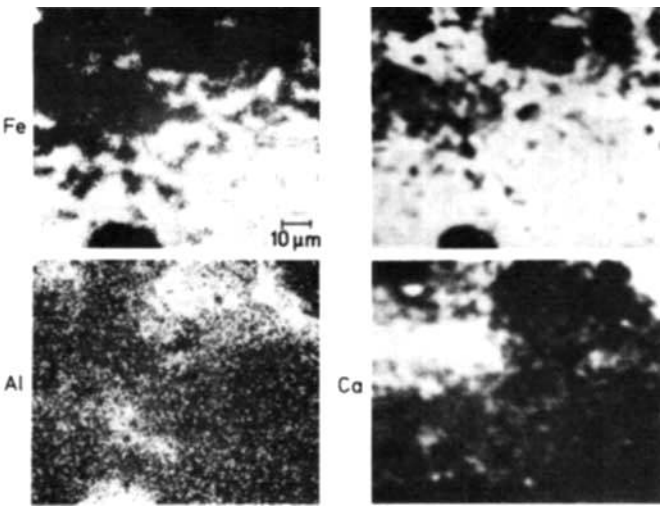

Fig. 3. 'Auger maps' showing the lateral distribution of the elements Fe, K, Al and Ca on the surface of an ammonia catalyst [5].

um is always found at locations where iron is also present. Although the total potassium concentration is only around 0.5%, its strong tendency to segregate out of the bulk leads to it covering about 30% of the metallic iron surface, where it serves as an 'electronic' promotor. More precisely, the catalytically active surface consists of metallic iron onto which a sub-monolayer amount of a two-dimensional K + O

phase (with a stoichiometry of about 1:1) is chemisorbed. This is certainly not one of the known bulk compounds of potassium, since these would be unstable under the reaction conditions.

Figure 4 depicts a high resolution transmission electron microscope (TEM) image of an activated catalyst particle, together with an electron diffraction pattern, at a selected location. The latter illustrates the single crystal character,

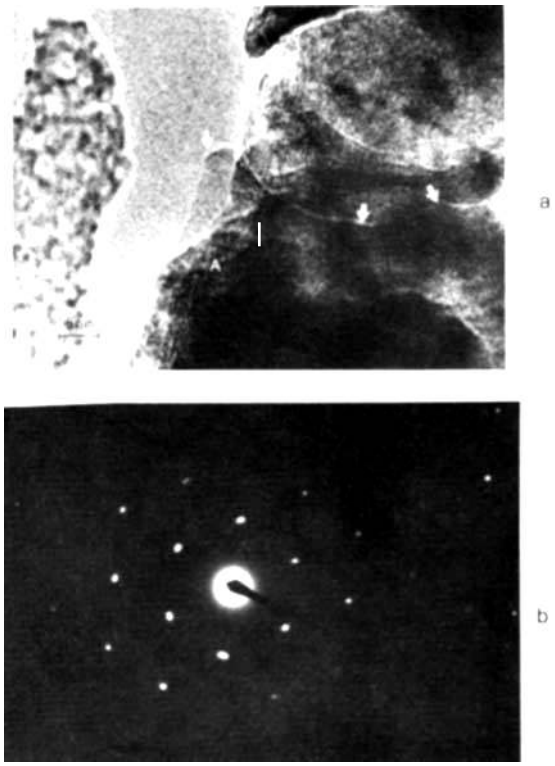

Fig. 4. a) Transmission electron microscope (TEM) image of an ammonia catalyst. Region A shows the lattice planes of a α-Fe lamella with (111) orientation. The arrows indicate the boundaries of this lamella within a stack of others having different orientations. The region on the left-hand side is amorphous carbon from the mounting support. b) Corresponding electron diffraction image, which can be identified as an iron single crystal (111) orientation [6].

which can be identified unambiguously as the (111) plane of α iron.[6] Closer inspection of the TEM image reveals the individual network layers and indicates that the catalyst primarily consists of small single crystallite particles of iron, the external surface of which, as we have previously seen, is partially covered with a K + O adsorption layer.

It therefore makes sense to use clean single crystal surfaces of iron with different orientations as a suitable model system for studying the influence of the atomic structure of the surface. The effect of electronic promotors can then be investigated via deliberate dosing with potassium.

Such samples have areas of at most 1 cm^2, so that measuring the conversion of a catalytic reaction represents a considerable experimental challenge. Despite this, *Somorjai* et al. were able to conduct such measurements successfully for a stoichiometric N_2:H_2 mixture at a pressure of 20 bar and a temperature of 500 °C.[8] They found that the activity varied between the various surface orientations by two orders of magnitude in the sequence (111) > (100) > (110), that is to say it was strongly influenced by the surface structure. However, even the Fe(111) surface exhibits only relatively low activity: the probability that a nitrogen molecule arriving at the surface will leave it as ammonia is only of the order of magnitude of one in a million.

The direct determination of chemisorbed complexes bound on the surface using the techniques of surface physics, requires, as mentioned above, a shift to much lower pressures ($\leq 10^{-3}$ mbar). Whether or not the surface species formed at high pressures remain stable under high vacuum depends on the temperature and the strength of the chemisorption bonding, and this has to be checked for each case individually. Provided one proceeds with adequate caution, however, surmounting the 'pressure gap' presents no problems in principle.

3. Elementary Processes in the Interaction between Molecules and Surfaces

Conceptually, a chemical reaction can be envisaged in its general form as the motion of a system of atoms along a 'reaction coordinate', in the course of which the energy changes in the manner shown in Figure 5. The local minima

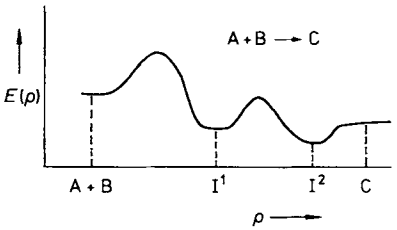

Fig. 5. Schematic diagram of the energy changes along the reaction coordinate ϱ for a chemical reaction (A + B → C). I = intermediate.

denote the nuclear configurations of intermediate compounds, while the maxima, representing the transition states, have to be overcome by summoning up the associated activation energy. Knowledge of the intermediates' properties and the rates of the respective transformations furnishes the reaction mechanism and, moreover, enables one to predict the total rate of the reaction. With the exception of the simplest gas phase reactions, a complete a priori theoretical evaluation is, however, still a long way off and one still has to rely on detailed experimental data.

The elementary processes in heterogeneously catalyzed reactions are as shown schematically in Figure 6: a molecule arriving at the surface can be bound (chemisorbed) there; the

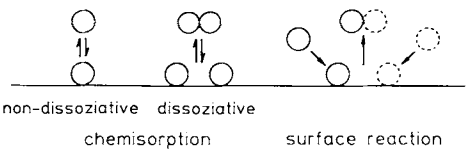

Fig. 6. Elementary processes in the interaction between molecules and a solid surface.

bonding process can be reversed and the molecule desorbed as a result of thermal activation. The surface bonding can also lead to bond rupture within the molecule (dissociative chemisorption), in which case desorption occurs via recombination of the fragments on the surface. Finally, the formation of new bonds can take place on the surface and, as a consequence of this, different molecules will then be desorbed.

It is obvious that the determination of the chemisorption complexes, together with the dynamics of their formation and transformation, is the key to understanding the elementary processes in a heterogeneously catalyzed reaction. Nowadays there is a whole variety of experimental methods available for such work.[9] These have recently been augmented in a spectacular fashion by the invention of scanning tunneling microscopy (STM) by *Binnig* and *Rohrer*.[10] Figure 7 illustrates the direct imaging of an Al(111) surface with

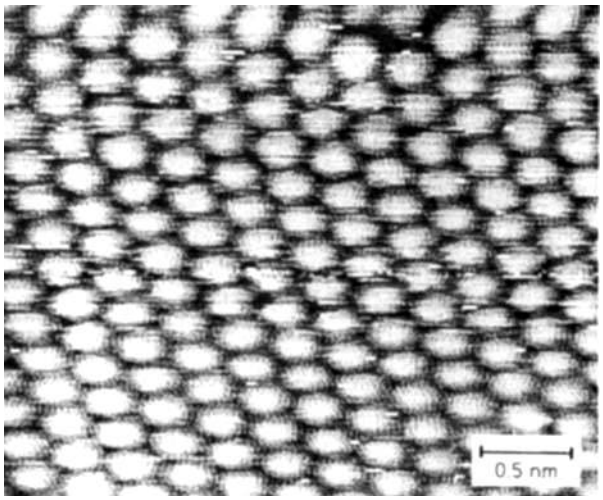

Fig. 7. Image of an Al(111) surface with atomic resolution obtained with the help of scanning tunneling microscopy [11].

atomic resolution as obtained by this technique.[11] Figure 8 shows the same surface with three chemisorbed C atoms.[12] One can see that these favor a coordination with three neighboring substrate atoms, i.e. they occupy defined adsorption sites.

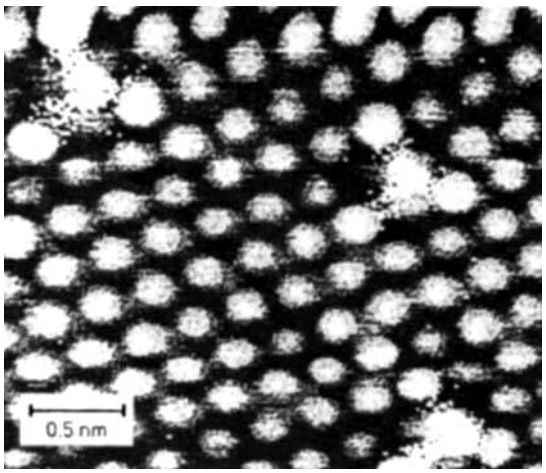

Fig. 8. Scanning tunneling microscope image of an Al(111) surface with three chemisorbed C atoms, which are discernible as diffuse light spots over a triangle of neighboring substrate atoms [12].

Generally, neighboring chemisorbed particles interact with each other, and this commonly gives rise to the formation of ordered two-dimensional phases. As an example, a sequence of STM images of a Cu(110) surface with increasing coverage of chemisorbed oxygen atoms is shown in Figure 9.[13] At low surface concentrations, small islands of a

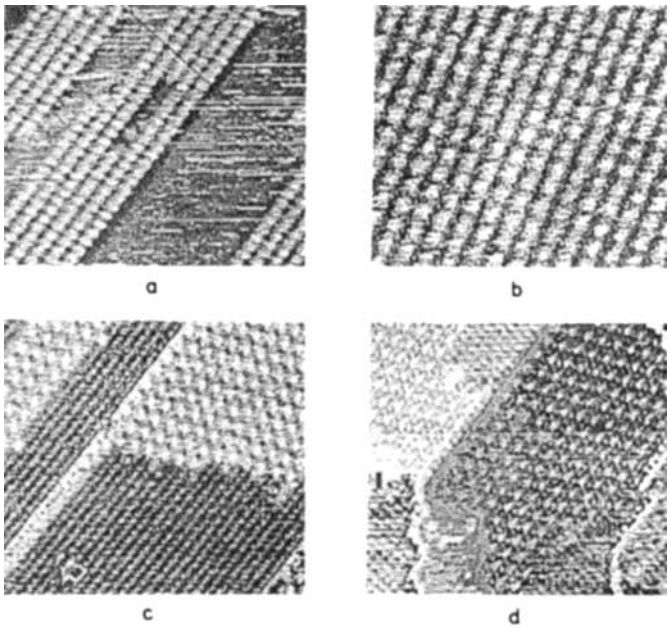

Fig. 9. Series of scanning tunneling microscope images of a Cu(110) surface with increasing O coverage [13]. a) Coverage $\theta < 1/2$: domains of a 2×1 phase together with patches of surface free from adsorbate. b) Fully developed 2×1 structure at $\theta = 1/2$. c) For $\theta > 1/2$: domains of a $c(6 \times 2)$ phase are formed in addition to the 2×1 phase (depicted as parallel streaks). d) Fully developed $c(6 \times 2)$ phase on terraces whose levels are separated by monatomic steps as differentiated by the gray scale.

2×1 phase are formed (a), which at higher concentrations cover the entire surface (b). Further increasing the degree of coverage leads to the formation of domains of an additional $c(6 \times 2)$ phase (c), rich in oxygen, which ultimately marks the saturation of the chemisorption phase (d) before the transition to three-dimensional oxide formation.

The actual structure of ordered surface phases can be determined by low-energy electron diffraction (LEED), a method which is analogous to X-ray diffraction for the determination of three-dimensional crystal structures. As an example, Figure 10 shows the structure of a 2×1 phase of chemisorbed oxygen atoms on a Ni(110) surface ascertained in this way[14] (this represents the counterpart to the previously depicted tunneling microscope image of the O-(2×1)/Cu(110) phase). The formation of chemisorption bonds has a profound influence on the substrate surface: every second row of atoms in the [001] direction is removed ('missing row' structure), that is to say the surface is reconstructed, and there is also an effect on the positions of atoms in deeper layers. Since the strength of the chemisorption bond is usually comparable to that between substrate atoms, it is entirely plausible that the most favorable overall atomic configuration may deviate considerably from that of the clean, i.e.

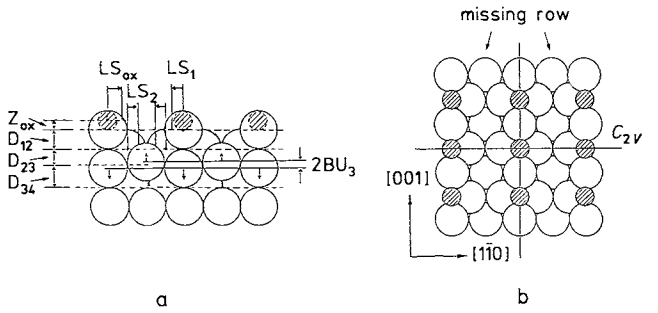

Fig. 10. Structural model of the 2×1 phase formed upon chemisorption of O atoms (shaded circles) on a Ni(110) surface [14]. Structural parameters: $Z_{ox} = 0.2$, $LS_{ox} = 0.1$, $LS_1 = 0.0$, $LS_2 = 0.0$, $D_{12} = 1.30$, $D_{23} = 1.23$, $D_{34} = 1.25$, $2BU_3 = \pm 0.05$ Å. a) Profile. b) Bird's-eye view.

adsorbate-free, surface. Conversely, there are a number of cases in which already the structure of clean surfaces deviates from the ideal bulk termination.[15]

In the above examples, the chemisorption phase was produced via the dissociative chemisorption of oxygen molecules, rather than by the action of oxygen atoms on the surface. This process is of decisive importance for catalysis, and can be rationalized with the aid of the schematic potential diagram shown in Figure 11. A molecule approaching

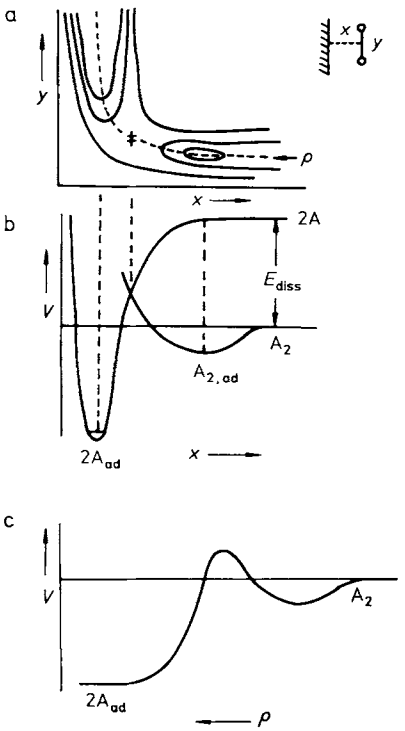

Fig. 11. Schematic potential diagram for dissociative chemisorption of a diatomic molecule A_2. a) Contour plot as a function of the distances x from surface and y between the two atoms. b) One-dimensional Lennard-Jones potential. c) Variation of potential along the reaction coordinate.

the surface experiences an initial decrease in its energy, can be weakly bound to the surface in the form of a molecular 'precursor', and will subsequently undergo dissociation when the activation barrier is surmounted. Since the formation of two bonds between the surface and the resultant two atoms more than compensates for the dissociation energy, the overall process involves a net energy gain. The course of the potential along the reaction coordinate and, in particular, the height of the activation barrier, determine the sticking coefficient, i.e. the probability that a molecule arriving at the surface will be chemisorbed dissociatively rather than bouncing back into the gas phase. Surface structure and coadsorbed particles, acting either as promotors or poisons, exert an appreciable influence at this juncture. As the rate constants of chemical reactions exhibit an exponential dependence on the activation energy, even slight energetic changes have a substantial effect on the kinetics.

4. Mechanism of Ammonia Synthesis

Let us now return to the problem of catalytic ammonia synthesis for a while. Figure 12 illustrates the increase in the surface concentration of atomically adsorbed nitrogen as a function of the nitrogen supply in the gas phase for the three low-index single-crystal surfaces of iron.[16] 1 L =

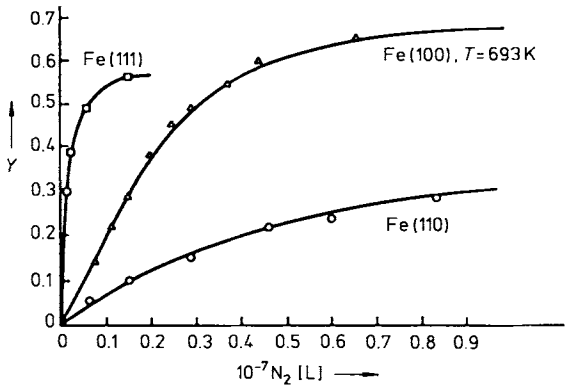

Fig. 12. Increase in surface concentration of chemisorbed N atoms (Y, in relative units) on Fe(111), (100), and (110) surfaces at 420 °C as a function of the exposure to N_2 molecules from the gas phase [16].

10^{-6} mbar s is a convenient unit for the gas exposure, because it suffices for the saturation of a surface with adsorbed particles if the sticking coefficient equals unity. Two features can be recognized from Figure 12: 1) the rate of dissociative nitrogen chemisorption depends strongly on the surface structure according to the sequence (111) > (100) > (110); 2) since typically not 1 L but $> 10^6$ L N_2 are necessary to achieve saturation, the sticking coefficient must be very low, i.e. of the order of 10^{-6}. Both findings are in full agreement with the results mentioned above concerning the catalytic activity of iron single crystal surfaces in ammonia formation, and demonstrate that the rate of ammonia synthesis is limited by the dissociative chemisorption of nitrogen. The agreement is all the more remarkable when one considers that the reaction conversions were measured at 20 bar and the chemisorption at 10^{-7} bar—the 'pressure gap' thus presents no serious hurdle in this case.

As the Fe(111) surface exhibits the highest activity, the interaction of nitrogen on this surface has been examined in

greatest detail. It has been shown that three different forms of adsorbed nitrogen can arise in this case, which may be characterized using the differing 'fingerprints' in the N_{1s}-photoelectron spectrum[17] (Fig. 13a): 1) a very weakly bound molecular state (γ), with terminal coupling[18] and a N-N stretching vibration at 2100 cm^{-1}, close to the value for the free molecule;[19] 2) under mild thermal activation, the γ-state is transformed into another molecular form (α), which is also directly populated from the gas phase and represents the actual 'precursor' for dissociative chemisorption.[20] The frequency of N-N stretching is much reduced (ca. 1500 cm^{-1}) signaling a pronounced weakening of the N–N bond.[17, 19, 21] The molecular axis is tilted with respect to the surface, so that an interaction with both nitrogen atoms occurs;[17, 18] 3) from the above state, the final dissociation ensues upon surmounting a modest activation barrier, yielding the strongly bound, atomic β form, as illustrated schematically in the potential diagram in Figure 13b.

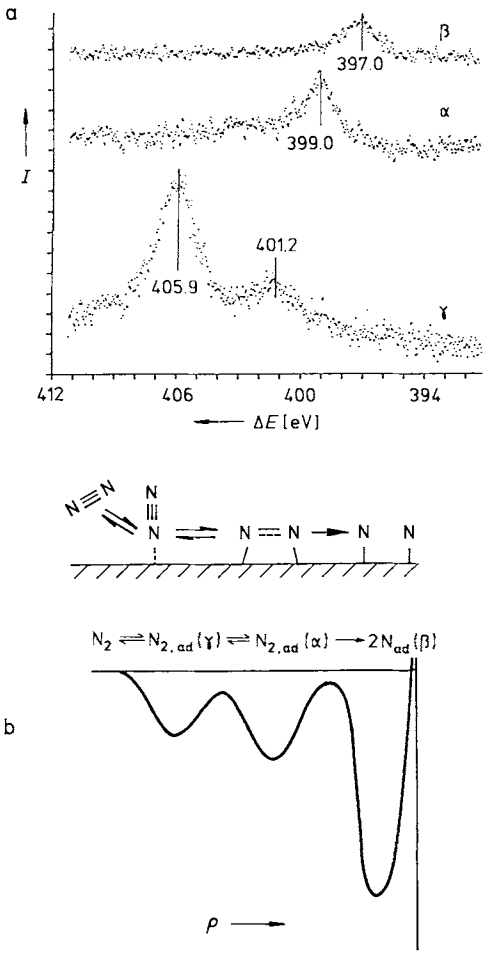

Fig. 13. N-1s photoelectron spectra of the various adsorbed N species on a Fe(111) surface (a) and the corresponding schematic potential (b) [17]. I = intensity; α,γ = molecular states; β = atomic state; $\Delta E = E - E_{Fermi}$; ϱ = reaction coordinate.

An example of a structure formed by chemisorbed N atoms on a Fe(100) surface is illustrated in Figure 14.[22] The nitrogen atoms occupy sites with fourfold coordination and, additionally, exhibit a strong interaction with the Fe atoms of the second layer. In other cases, the formation of the chemisorbed nitrogen phase is associated with considerable reconstruction of the substrate (see Section 3). Such phases can generally be denoted as 'surface nitrides' (the familiar bulk nitrides are thermodynamically unstable under the conditions of the ammonia synthesis!). *Mittasch*'s speculation that "in the catalytic formation of ammonia some kind of intermediate nitrides" arise, is thus entirely vindicated in its essence.

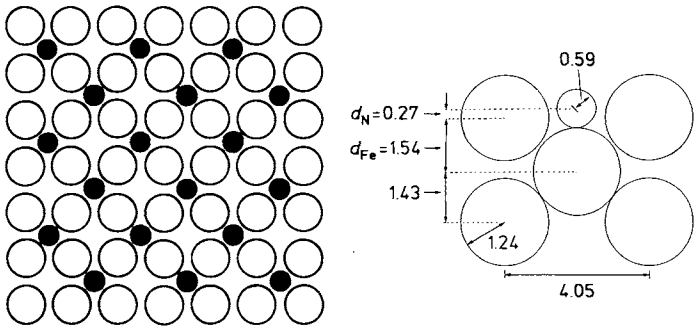

Fig. 14. Structural model of the c(2 × 2) phase formed by chemisorbed N atoms on an Fe(100) surface [22]. d = layer separation.

The role played by 'electronic' promotors can be studied by application of sub-monolayer amounts of potassium to pure iron surfaces. In this manner, it was shown that the sticking coefficient for dissociative nitrogen chemisorption could be raised dramatically.[23] This is essentially due to the increased substrate electron density in the vicinity of an adsorbed $K^{\delta\oplus}$ atom, which leads to a stabilization of the molecular α-state through increased π-back donation. This state (α_2) has a higher adsorption energy and the frequency of the N-N vibration is further lowered, thus facilitating dissociation.[21, 23–25]

The occurrence of various binding states for nitrogen on a potassium doped Fe(111) surface is manifested also in the thermal desorption spectrum, which exhibits maxima at the respective desorption temperatures (Fig. 15, curve a).[19] For

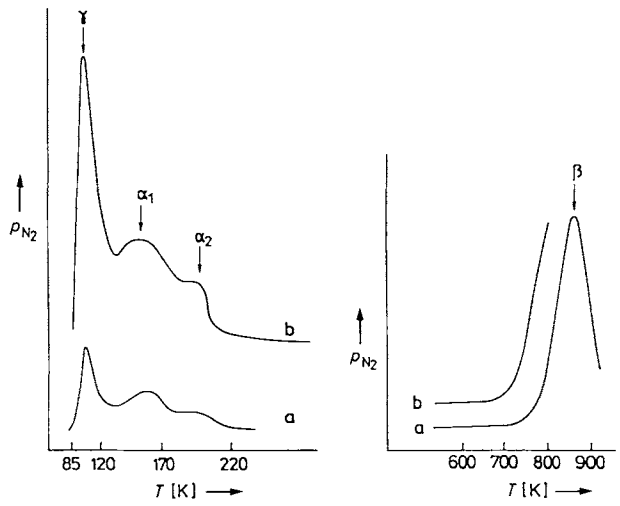

Fig. 15. Thermal desorption of N_2 from a K covered Fe(111) surface (curve a) and from a commercial ammonia catalyst (curve b) [19]. Left: desorption from the molecular states γ,α_1 and α_2. Right: Desorption following recombination of the atomic state β.

comparison, this figure depicts (curve b) data determined upon heating a nitrogen covered industrial catalyst.[26] It is notable that the temperature maxima, i.e. the respective bond energies, are in full agreement with one another. This demonstrates that the adsorption behavior of the commercial catalyst is simulated really well by the model system (Fe(111) surface, covered with around 1.2×10^{14} K atoms/cm^2). It further shows that the 'materials gap' mentioned above can be overcome in this case, and thus that the information obtained from surface science studies can form a basis for the *quantitative* modeling of 'real' catalysis in its own right.

The quintessential features of the results obtained from a large number of detailed studies on the individual steps of the catalytic ammonia synthesis are summarized in the energy diagram shown in Figure 16:[7, 27] the homogeneous reac-

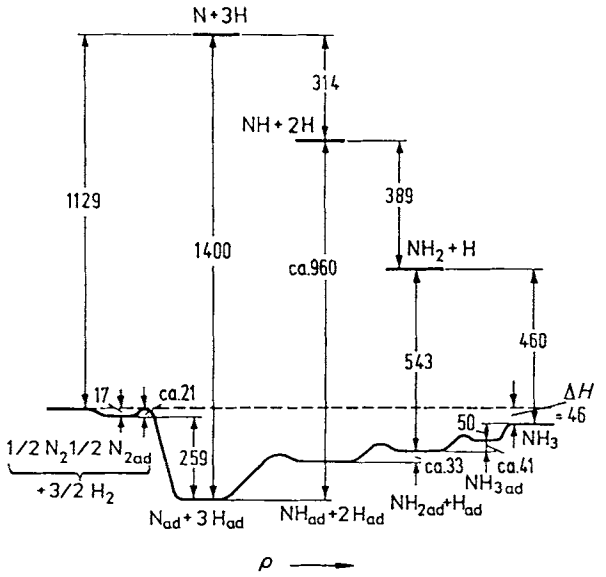

Fig. 16. Schematic potential diagram for the course of catalytic ammonia synthesis along the reaction coordinate in comparison to the energy differences for the corresponding non-catalytic steps (energy in kJ mol^{-1}) [7, 27].

tion in the gas phase would require a prohibitive amount of energy for the dissociation of the H_2 and N_2 molecules. In the presence of the catalyst, on the other hand, this process may be achieved by overcoming only relatively low energy barriers, the formation of chemisorbed nitrogen and hydrogen atoms actually even producing surplus energy. The further reaction steps comprise the successive recombination of N_{ad} and H_{ad}, ending with the desorption of NH_3. The corresponding energy demands of these elementary processes are easily met by virtue of the high reaction temperature ($\geq 400\,^{\circ}C$).

The attempt to predict the conversion in high-pressure industrial reactors using commercial catalysts on the basis of detailed information about the kinetic parameters for the individual steps, as obtained from the single-crystal model systems under the high vacuum conditions described, has been tackled by several research groups employing differing approaches.[28-29] As is evident from Figure 17, the agreement, e.g. in the analysis by *Stoltze* and *Nørskov*,[28] is really surprisingly good. This example illustrates that catalysis is

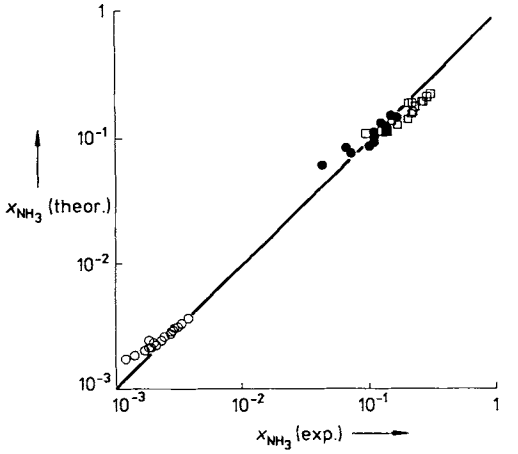

Fig. 17. Comparison of the ammonia yields determined experimentally under industrial conditions with theoretical values calculated with the help of model studies on a single surface. Taken from *Stoltze* and *Norskov* [28]. x = mol fraction. ○ = 1 atm, ● = 150 atm, □ = 300 atm.

by no means a 'black art', and that even complex technical systems can be described quantitatively via an analysis of the underlying elementary processes.

5. Nonlinear Dynamics: Temporal and Spatial Intrinsic Organization

The possibility of being able to calculate exactly the rate of a chemical reaction from a detailed knowledge of the kinetic parameters (i.e. reaction order and rate constants) for the individual steps, can admittedly, in certain cases, come up against fundamental limitations having their origins in the mathematical structure of the underlying equations.

For a catalytic reaction taking place in a continuous flow reactor, an open system well-removed from equilibrium is involved, the temporal behavior of which can be described by a series of coupled, nonlinear differential equations for the individual concentration variables (in our case the coverages by the various species), hence the expression 'nonlinear dynamics'. Systems of this kind need not behave in a stationary (i.e. time-independent) manner, even when external parameters (temperature, pressure) are maintained at constant levels, but can undergo transitions to temporal and spatial self-organization. Such phenomena were classified as 'dissipative structures' by *Prigogine* et al.[30] and were later incorporated into the general area of synergetics by *Haken*.[31]

Temporally oscillating reaction rates were observed early on in detail, e.g. with the Belousov-Zhabotinsky (BZ) reaction in homogeneous solution[32] and with electrochemical systems.[33] Such effects were first described for a heterogeneously catalyzed reaction, CO oxidation on supported Pt catalysts, by *Wicke* et al. about twenty years ago.[34] Here too, the reaction mechanism could be clarified using the strategy described.

For Pt(100) and Pt(110) single crystal surfaces at low partial pressures and under strictly isothermal conditions, the presence of CO triggers a structural transformation of the surface, with an associated increase in the sticking coefficient

for oxygen. In this way, the adsorbed CO is removed by reaction with a high probability and the surface reverts to its original structural modification. Under certain conditions, the surface can thus alternate between two states with high and low activities, giving rise to corresponding oscillations in the reaction rate. As an example, Figure 18 shows for a Pt(110) surface the development of regular oscillations following a rapid change of the O_2 partial pressure to a new value at the point marked by the arrow.[37]

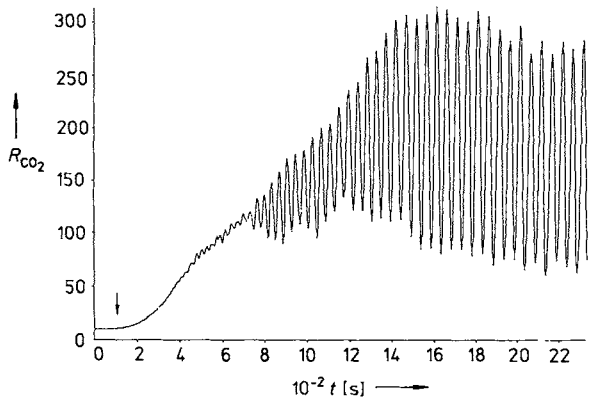

Fig. 18. Rate R_{CO_2} of catalytic CO_2 formation on a Pt(110) surface (in arbitrary units) as a function of time under steady-state flow conditions [37]. $T = 470$ K, $p_{CO} = 3.0 \times 10^{-5}$ mbar, at the point indicated by the arrow, p_{O_2} was raised from 2.0×10^{-4} to 2.6×10^{-4} mbar.

The occurrence of such oscillations is usually restricted to a certain range of values for the external parameters. In the example shown in Figure 19, small amplitude oscillations commence upon adopting a particular value of the CO partial pressure ($p_{CO} = 5.6 \times 10^{-5}$ mbar) (a). The amplitude initially grows upon further reduction of p_{CO}, while the frequency remains unchanged (b); this signals the occurrence of a so-called Hopf bifurcation. Reducing the CO partial pressure still further leads to a doubling of the period (i.e. with alternating large and small amplitudes) (c), which is then itself superseded by a further doubling (not shown here). Finally, at $p_{CO} = 5.2 \times 10^{-5}$ mbar, irregular dynamic behavior is observed. A detailed analysis[38] indicated that this reflects a transition to deterministic chaos via the so-called Feigenbaum route.[39] In contrast to the regular oscillations, the dynamic behavior is no longer predictable, hence the term 'chaos'. This effect occurs *despite the fact* that the external conditions, and thus also the mathematical formulation, are well defined (apart from small stochastic fluctuations, which can never be eliminated entirely), hence the adjective 'deterministic'.

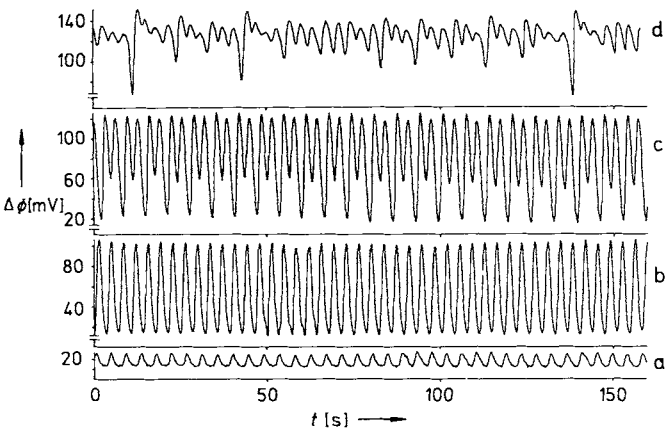

Fig. 19. Various forms of oscillation encountered during the catalytic oxidation of CO on a Pt(110) surface under steady state conditions. $T = 530$ K, $p_{O_2} = 1.1 \times 10^{-4}$ mbar, p_{CO} was varied between 5.6×10^{-5} (a) and 5.2×10^{-5} mbar (d) [37].

Chaotic phenomena occur in totally different areas and have shaken the scientific credo of being able, in principle anyway, to predict the temporal behavior of *macroscopic* systems.

The system under consideration exhibits a further peculiarity: the manifestation of temporal variations in the reaction rate integrated over the entire surface of 30 mm^2 necessitates some form of communication between different locations, i.e. an additional, spatial self-organization. For the Belousov-Zhabotinsky reaction mentioned earlier, local variations in concentration can be rendered visible by means of color differences, and manifest themselves, for example, as expanding concentric rings or spirals[40]. With the system just described, corresponding differences in CO and O coverages can be visualized using a recently developed photoemission electron microscope for which the contrast is determined by variations in the (local) work function associated with the dipole moments of the adsorbates. Two examples of the numerous different patterns formed (the phenomenology of which is dictated uniquely by temperature and partial pressure) are shown in Figure 20, corresponding to the rings and spirals of the BZ reaction mentioned earlier. It should once again be stressed that these patterns are truly two-dimensional. The contrast is created only by local differences in the coverage on an initially homogeneous surface (dark: O_{ad} coverage; bright CO_{ad} coverage). The patterns change on a time scale of about 1 s (sometimes much more rapidly too); when conditions are no longer suitable (e.g. one of the gases is cut off) the patterns disappear immediately and the surface once again assumes a fully uniform appearance.

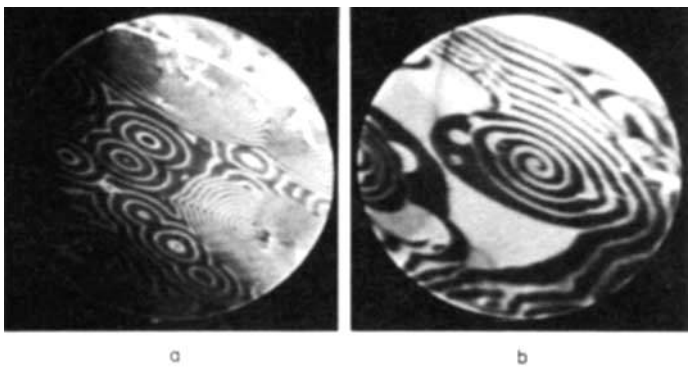

Fig. 20. Spatio-temporal pattern formation on a Pt(110) surface during the oscillatory CO oxidation. Both figures depict a section of the surface with a diameter of approximately 0.5 mm as imaged by photoemission electronmicroscopy [41]. a) $T = 430$ K, $p_{O_2} = 3.2 \times 10^{-4}$ mbar, $p_{CO} = 3.0 \times 10^{-5}$ mbar. b) $T = 435$ K, $p_{O_2} = 3.0 \times 10^{-4}$ mbar, $p_{CO} = 2.8 \times 10^{-5}$ mbar.

6. Conclusion

In this paper, an attempt has been made to show how, even for a phenomenon as complex as heterogeneous catalysis, basic research can enable one to proceed to underlying fundamental principles. This route and its likely future relevance for practical applications was formulated by *Mittasch* several decades ago as follows:[41]

"When one considers that catalysis is truly a 'land of unlimited possibilities', one cannot exclude the likelihood that continued experimental research will not only provide complete theoretical explanations, but could also become of importance in the further refinement of commercial processes."

Received: April 18, 1990 [A 785 IE]
German version: *Angew. Chem. 102* (1990) 1258

[1] a) Mittasch: *Geschichte der Ammoniaksynthese*, Verlag Chemie, Weinheim 1951; b) [1a], p. 116.
[2] [1a], p. 92.
[3] C. Bosch, A. Mittasch, G. Stern, H. Wolf, DRP 249447 (1910) with additions DRP 258146 and 262823, BASF.
[4] [1a], p. 111/112.
[5] G. Ertl, D. Prigge, R. Schlögl, M. Weiss, *J. Catal. 79* (1983) 359.
[6] R. Schlögl in: J. R. Jennings (Ed.): *Catalytic Ammonia Synthesis*, Plenum, New York 1990, in press (Chapter 2).
[7] G. Ertl in [6], Chapter 5.
[8] a) N. D. Spencer, R. C. Schoonmaker, G. A. Somorjai, *J. Catal. 74* (1982) 129; b) D. D. Strongin, J. Carrazza, S. R. Bare, G. A. Somorjai, *ibid. 103* (1987) 213.
[9] a) G. Ertl, J. Küppers: *Low Energy Electrons and Surface Chemistry*, 2nd Edit., VCH, Weinheim 1985; b) D. P. Woodruff, T. A. Delchar: *Modern Techniques of Surface Science*, Cambridge University Press, Cambridge 1986; c) A. Zangwill: *Physics at Surfaces*, Cambridge University Press, Cambridge 1988.
[10] See, e.g., H. Rohrer, N. Garcia, R. J. Behm (Eds.): *Basic Concepts and Applications in Scanning Tunneling Microscopy*, Kluver, Dordrecht 1990; b) G. Binnig, H. Rohrer, *Angew. Chem. 99* (1987) 622; *Angew. Chem. Int. Ed. Engl. 26* (1987) 606.
[11] J. Wintterlin, J. Wiechers, H. Brune, T. Gritsch, H. Höfer, R. J. Behm, *Phys. Rev. Lett. 62* (1988) 59.
[12] H. Brune, J. Wintterlin, R. J. Behm, G. Ertl, *Europhys. Lett. 13* (1990) 123.
[13] D. Coulman, J. Wintterlin, R. J. Behm, G. Ertl, *Phys. Rev. Lett. 64* (1990) 1761; *Surf. Sci.*, in press.
[14] G. Kleinle, J. Wintterlin, G. Ertl, R. J. Behm, F. Jona, W. Moritz, *Surf. Sci. 225* (1990) 171.
[15] K. Müller, *Ber. Bunsen-Ges. Phys. Chem. 90* (1986) 184.
[16] a) F. Boszo, G. Ertl, M. Grunze, M. Weiss, *J. Catal. 49* (1977) 18; b) F. Boszo, G. Ertl, M. Weiss, *ibid. 50* (1977) 519.
[17] M. Grunze, M. Golze, W. Hirschwald, H. J. Freund, H. Pulm, U. Seip, M. C. Tsai, G. Ertl, J. Küppers, *Phys. Rev. Lett. 53* (1984) 850.
[18] H. J. Freund, B. Bartos, R. P. Messmer, M. Grunze, H. Kuhlenbeck, M. Neumann, *Surf. Sci. 185* (1987) 187.
[19] L. J. Whitman, C. E. Bartosch, W. Ho, G. Strasser, M. Grunze, *Phys. Rev. Lett. 56* (1986) 1984.
[20] G. Ertl, S. B. Lee, M. Weiss, *Surf. Sci. 114* (1982) 515.
[21] M. C. Tsai, U. Seip, I. C. Bassignana, J. Küppers, G. Ertl, *Surf. Sci. 155* (1985) 387.
[22] R. Imbihl, R. J. Behm, W. Moritz, G. Ertl, *Surf. Sci. 123* (1982) 129.
[23] G. Ertl, S. B. Lee, M. Weiss, *Surf. Sci. 114* (1982) 527.
[24] L. J. Whitman, C. E. Bartosch, W. Ho, *J. Chem. Phys. 85* (1986) 3688.
[25] a) N. D. Lang, S. Holloway, J. K. Nørskov, *Surf. Sci. 150* (1985) 24; b) J. K. Nørskov, in H. P. Bonzel, A. M. Bradshaw, G. Ertl, (Eds.): *Alkali Metal Adsorption*, Elsevier, Amsterdam 1989, p. 253.
[26] R. Schlögl, R. C. Schoonmaker, M. Muhler, G. Ertl, *Catal. Lett. 1* (1988) 237.
[27] G. Ertl in J. R. Anderson, M. Boudart (Eds.): *Catal. Sci. Technol. Vol. 4*, Springer, Berlin 1983, p. 209.
[28] P. Stoltze, J. K. Nørskov, *Phys. Rev. Lett. 55* (1985) 2502; *Surf. Sci. 117* (1988) L230; *J. Catal. 110* (1988) 1.
[29] a) M. Bowker, I. Parker, K. Waugh, *Appl. Catal. 14* (1985) 101, with revision in *Surf. Sci. 197* (1988) L223; b) J. A. Dumesic, A. A. Trevino, *J. Catal. 116* (1989), 119.
[30] G. Nicolis, I. Prigogine: *Self-Organisation in Nonequilibrium Systems*, Wiley, New York 1977, See also I. Prigogine, *Angew. Chem. 90* (1978) 704.
[31] H. Haken: *Synergetics. An Introduction*, Springer, Berlin 1982; *Advanced Synergetics*, Springer, Berlin 1983.
[32] See, e.g., A. M. Zhabotinsky, *Ber. Bunsen-Ges. Phys. Chem. 84* (1980) 303.
[33] See, e.g., U. F. Franck, *Ber. Bunsen-Ges. Phys. Chem. 84* (1980) 334.
[34] a) P. Hugo, *Ber. Bunsen-Ges. Phys. Chem. 74* (1970) 121; b) H. Beusch, P. Fieguth, E. Wicke, *Chem. Ing. Techn. 44* (1972) 445.
[35] M. Eiswirth, K. Krischer, G. Ertl, *Appl. Phys. A 51* (1990) 79.
[36] G. Ertl, *Adv. Catal. 37* (1990), in press.
[37] M. Eiswirth, G. Ertl, *Surf. Sci. 177* (1986) 90.
[38] M. Eiswirth, K. Krischer, G. Ertl, *Surf. Sci. 202* (1988) 565.
[39] a) H. G. Schuster: *Deterministic Chaos*, Physik-Verlag, Weinheim 1984; b) J. M. T. Thompson, H. B. Stewart: *Nonlinear Dynamics and Chaos*, Wiley, New York 1987; c) S. Wiggins: *Global Bifurcations and Chaos*, Springer, Berlin 1988.
[40] R. J. Field, M. Burger (Eds.): *Oscillations and Travelling Waves in Chemical Systems*, Wiley, New York 1985.
[41] a) H. H. Rotermund, W. Engel, M. Kordesch, G. Ertl, *Nature (London) 343* (1990) 355; b) H. H. Rotermund, W. Engel, S. Jakubith, A. von Oertzen, G. Ertl, unpublished.
[42] A. Mittasch: *Chemische Grundlegung der industriellen Ammoniak-Katalyse – BASF-Versuche 1909–1912*. Printed as manuscript, Ludwigshafen 1953.